View Online / Journal Homepage / Table of Contents for this issue
Dynamic Article Links

Lab on a Chip

Cite this: *Lab Chip*, 2011, **11**, 3130

www.rsc.org/loc

PAPER

Microfluidic purification and analysis of hematopoietic stem cells from bone marrow

Romana Schirhagl,[a] Ingo Fuereder,[a] Eric W. Hall,[a] Bruno C. Medeiros[b] and Richard N. Zare*[a]

Received 26th April 2011, Accepted 8th July 2011
DOI: 10.1039/c1lc20353c

Hematopoietic stem cells are larger in size than other cells present in bone marrow, with the exception of monocytes. This distinguishing characteristic can be used to separate them from a whole-marrow sample. A microfluidic device was fabricated using an integrated membrane that is porous at defined areas. This allows for simultaneous valving and filtering functionality, which is crucial for preventing irreversible clogging. This device, as well as a separation procedure, was optimized in this work to enrich hematopoietic progenitor cells from diluted bone marrow of leukemia patients without any additional sample preparation. An enrichment of up to 98% was achieved with this method and the process was scaled up to 17.2 μL min^{-1} of processed sample. Additionally, stem cells were stained with specific antibodies for further analysis. Using a custom-made computer program, the filter was scanned to characterize and quantify cells based on fluorescence. The results were evaluated by comparing them against the results obtained from flow cytometry, confocal microscopy, and Coulter counting.

Introduction

Therapies based on stem cells have been one of the most documented approaches in regenerative medicine and promise treatment for a multitude of diseases and disorders. To study further these cells, their interactions, and their behavior, as well as their abundance correlated with pathogenic conditions, it is necessary to isolate them.[1] However, the ex vivo expansion of stem cells and their *in vivo* delivery are restricted by the limited availability of stem cell sources.[2,3]

We believe that microfluidics can be used to effectively filter stem cells from samples based on their size. Microfluidics offers the ability to handle small volumes and apply defined, directed flows.[4] It can also be coupled with numerous analytical techniques such as optical[5,6] or acoustic detection,[7] mass spectrometry,[8] dielectric spectroscopy,[9] or surface plasmon resonance (SPR).[10] These facts make microfluidic platforms rather ideal for handling and studying cells. It has already been shown that microfluidics can be used to purify cells by magnetic forces[11] or by methods based on fluorescence.[12] However, these methods suffer from the fact that multiple cells cannot be sorted simultaneously and thus the extent to which these processes can be scaled up is limited. Additionally, expensive labels (magnetic or fluorescent), complex apertures, or time-consuming sample preparation are required. Huang *et al.*[13] have presented a deterministic lateral displacement method which shows excellent size resolution of polymeric particles. However, this method has only been used for rigid beads that are an order of magnitude smaller than cells and the high pressures required for separation (30 kPa) may limit its use for cell sorting because of possible cell damage. Field-flow fractionation is an appealing alternative for sorting highly abundant cells like red blood cells.[14] However, because the sample is diluted during the separation and only a small volume (15 μL) can be separated at a time this method is not applicable for sorting rare stem cells.

Filters are an attractive alternative for microfluidic-based cell sorting because they are relatively inexpensive, do not require any labels, and it is possible to process large numbers of cells in a short amount of time.[15] However, filter-based devices often suffer from irreversible clogging and the inability to incorporate valves.[15,16] One way to circumvent this problem is to use a membrane that is only porous in specifically defined areas so the membrane simultaneously acts as both a filter and a valve. Such a device was designed by our group[17,18] where a PDMS membrane with pores in defined areas, first developed by the Whitesides group,[19] was incorporated into a microfluidic chip. The dual function of the membrane allows the chip's user to stop irreversible clogging by alternately flushing and filtering. This device was previously tested with polystyrene beads and blood samples that were artificially enriched with large cells. In this work, we have improved the device and optimized it for the important purpose of sorting hematopoietic stem cells from bone marrow.

[a]*Department of Chemistry, Stanford University, Stanford, California, 94305-5080, USA. E-mail: zare@stanford.edu; Fax: +1 650 725-0259; Tel: +1 650 723-3062*
[b]*Department of Medicine, Stanford University, Stanford, CA, 94305-5821, USA*

Experimental details

Materials

Fluorescein isothiocyanate (FITC) mouse anti CD34 human antibodies (binding to progenitor cells) were purchased from BD Pharmingen and used as suggested by the company. According to Berenson *et al.*[20] all hematopoietic progenitors detected by *in vitro* assays are CD34+.

As given by the vendor (BD Pharmingen) anti CD34 antibodies react with a single chain 105–120 kDa heavily o-glycosylated transmembrane glycoprotein expressed on hematopoietic progenitor cells. Strictly, only cells that are CD34+, CD38− and Lin− are considered hematopoietic stem cells. Cells that express only CD34 and CD38 are immature hematopoietic cells with some, although limited, self-renewal capacity. So there might be some cross selectivity to vascular endothelium and some tissue fibroblasts; however, these are typically smaller than stem cells. Bone marrow sample taken from patients with acute leukemia was provided by the Stanford Cancer Center (IRB 18329). CellTracker Orange dye (5-(and-6)-(((4-chloromethyl)-benzoyl) amino)tetramethylrhodamine) was ordered from Invitrogen (Molecular Probes) and used for viability tests as suggested by the vendor. Polydimethylsiloxane (PDMS) was obtained from RS Hughes. All other chemicals were purchased in highest or analytical grade from Sigma Aldrich or VWR.

Fabrication of the microfluidic chips

A three-layer design was chosen to generate a sorting device that can simultaneously valve and filter. The top and bottom layers contain channels and valve-control architecture, while the middle layer is a membrane that acts as both a filter and a valve. The membrane was fabricated by spin coating PDMS, diluted with cyclohexane, on a silicon master mold with photoresist posts.[17] PDMS:crosslinker in the ratio 5 : 1 was poured on a wafer with the desired channel structure for the top layer and a PDMS: crosslinker in the ratio 20 : 1 for the bottom layer. After curing for 1 h at 80 °C inlets to top layer channels are punched and the top layer is aligned to the membrane. 5 : 1 PDMS:crosslinker is poured around the chip and followed by curing for 1 h at 80 °C to achieve bonding. The top-layer is peeled off from the wafer together with the membrane and inlets connecting to the bottom layer channels are punched. Finally, these two are aligned to the bottom layer and cured another hour at 80 °C (different-ratio bonding).[20] Detailed fabrication procedures can be found in the work by Wei *et al.*[18] Fig. 1c depicts a top-down view of the filter-containing separation area of the assembled chip in the original round design.

Prior to chip fabrication, three different silicon master molds were prepared using standard photolithography techniques. For the most crucial part of the device, the porous membrane, a wafer was developed with posts made of SU-8 that were 20 μm in height and varied in diameter depending on the pore size desired. Fig. 1b shows a scanning electron microscopy (SEM) image of such a post. The optimal thickness of the membrane must be less than this 20 μm limit in order to obtain through holes, but thick enough to be mechanically robust. The spin coating speed and dilution factor of the prepolymer are critical in this regard, and their optimization has been studied previously.[18]

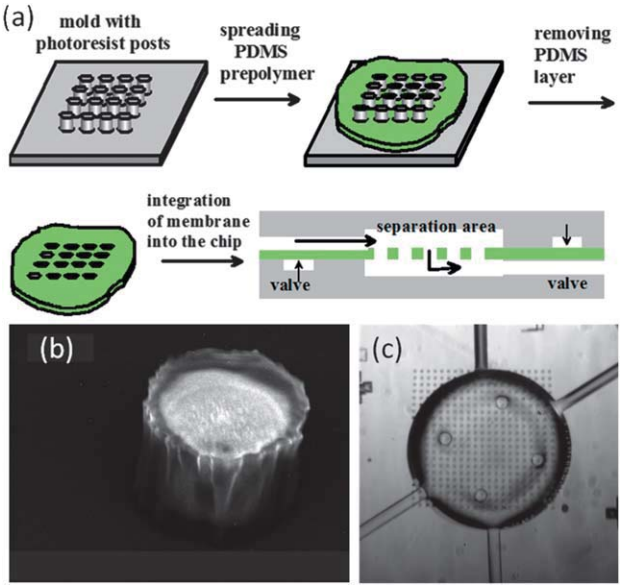

Fig. 1 Fabrication of a microporous membrane and its integration into a microfluidic chip. (a) Photoresist posts (SU-8) are created on a silicon wafer by standard photolithography. A PDMS membrane is cast onto the wafer and peeled off when curing is complete. After integration into the chip, the membrane is used as both a filter as well as a valve. (Application of pressure on one side of the membrane closes the channel on the other side) (b) SEM image of an SU-8 post 18 μm wide and 20 μm high. (c) image of the separation area of the assembled particle-sorting chip.

Because hematopoietic stem cells are so rare, it is important to be able to handle relatively large amounts of fluid to achieve a significant sample size. Therefore, a large separation area is desired to process these volumes efficiently. However, it is not sufficient to simply use a larger version of the original circular shaped filter design[18] owing to fabrication limitations. Large, unsupported membrane areas tend to collapse, sealing those areas of the filter from use. An improvement upon the previous design was achieved by replacing the circular design of the separation area with a parallelogram, which can be enhanced by extending the area of the filter in the longitudinal direction. The method used to filter cells with this device is shown in Fig. 2a and a photo of the chip colored with food dye is depicted in Fig. 2b. Valves are colored in red while the flow channels and filter are both colored in green. Fig. 2c and 2d demonstrate a performance comparison of the circle- and parallelogram-based designs. The throughput of the parallelogram configuration is six times greater than the circular configuration.

Performing a separation

Prior to cell sorting, the valve-control architecture is filled with water pressurized between 5 and 10 psi. 40 μL of 1 : 40 diluted bone marrow in phosphate buffered saline (PBS) are injected into a channel in the top layer. The flow directs small particles through the filter to the bottom layer and produces what we will refer to as the 'bottom fraction.' Everything that does not pass through the pores is trapped on the filter and stays in the top layer, and will thus be called the 'top fraction.' During this step, the green valves in Fig. 2a are opened and the red ones are closed.

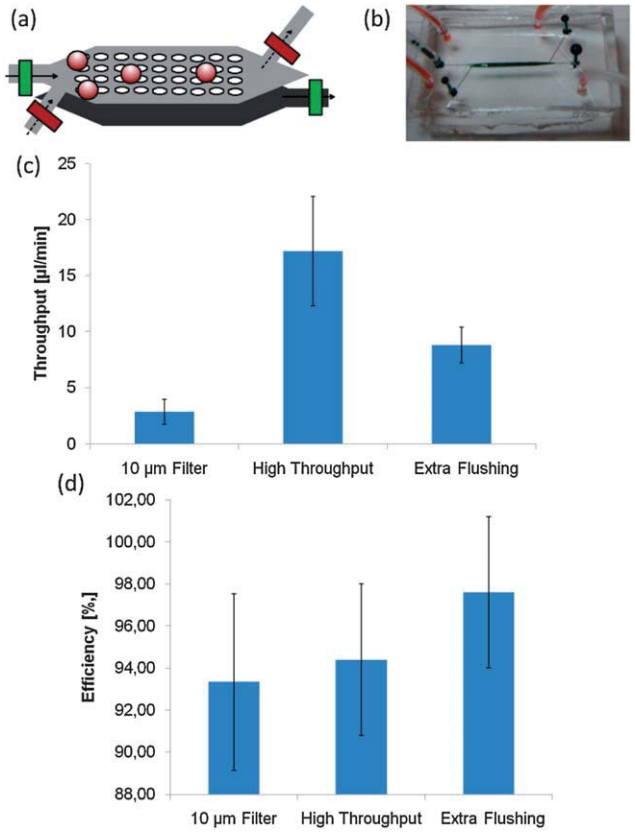

Fig. 2 Schematic and evaluation of sorting procedure using parallelogram-shaped separation area. (a) Scheme of the sorting procedure. The green valves are left open when the sample is injected. Particles that are larger than the pore size are trapped on the filter whereas smaller ones can pass through. If particles become trapped on the filter, the green valves are closed and a cross-flow is applied through the beveled channels by opening the red valves. The parallelogram shape of the separation area allows us to enhance the throughput by a factor of 6. (b) shows the chip itself. The valves and the main channel were visualized by red and green food dye respectively. (c) and (d) show the throughput (which means time that is needed to get a certain volume of sample including the chip handling) and separation efficiency, respectively, of this chip (second column) compared to the original one devised in our lab by Wei *et al.* (first column). The third column corresponds to an experiment were the purity of the large cells was improved by introducing one extra flushing step. Buffer was inserted in the same direction as the sample was injected before proceeding with the separation.

The bottom fraction is extracted from the outlet (on the right in Fig. 2a) and the green valves are closed. The top fraction is removed by flushing the membrane area from the angled side channels. Then, the green valves are closed and the red ones are opened. By flushing the device in the angled direction, irreversible clogging of the filter was prevented, which is crucial for separating larger volumes without sacrificing much yield. This new design is capable of processing larger sample volumes (100–200 µL compared to 40–50 µL) before flushing is required. In prior experiments this volume was limited by a lower throughput, and thus a longer processing time, which allowed for cells to sediment at the inlets and clog the channel.

If a higher purity is desired, optional intermittent washing steps can be introduced. In these steps, an aliquot of buffer is washed through the main channel between separations before flushing through the angled channels. This washing step forced small cells through the filter that did not make their way to the separation area and would otherwise be flushed out with the top fraction. The improvement to purity (and the sacrifice to throughput) gained by this step is shown in Fig. 2c and 2d.

On-chip detection and quantification of cells

Separations are relatively fast (up to 17.2 µL min^{-1} obtained with the high throughput design; see Fig. 2) and can be performed without any sample preparation or labelling. However, if on-chip identification and quantification is desired, the cells can be labelled prior to separation. To evaluate our method, FITC mouse anti CD34 human antibodies were used to fluorescently label hematopoietic stem cells. In order to quantify the number of cells on the membrane, an image of an area of the membrane was taken using a CCD camera (Mintron MTV-63KR11N) and an inverted microscope (Nikon Eclipse TE2000-U). The brightness of the pixels corresponds to photon counts on a particular area of the CCD chip. The number of pixels exceeding an empirically determined threshold was counted as a particle. The laser (Crysta Laser max. output power: 495 mW, 633 nm) was expanded *via* an optical set-up to cover an area of approximately 400 µm × 400 µm within the separation device, which can be regarded as the detection area. The device was placed on a precisely movable stage (Lstep Märzhäuser) which was controlled remotely. A Labview (National Instruments) program built in-house allowed us to perform a raster scan in order to cover the whole separation area systematically. Additionally, the camera control was synchronized to this scanning movement in such a way that we automatically obtained a composite fluorescence image of the entire separation area. After appropriate calibration (see Fig. 3), this automated scanning procedure allowed us to achieve a rapid and reliable quantification of the cells caught on the membrane.

Viability test of cells after sorting

A viability test of cells processed by the device was performed with CellTracker Orange CMTMR. This was done to confirm

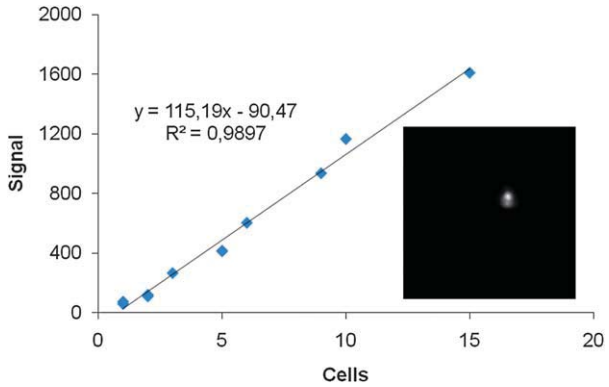

Fig. 3 Calibration for automated stem cell counting. The signal corresponding to the number of pixels containing a brightness over a certain threshold was correlated with the number of cells *via* manual counting. The inset shows an image of a stem cell taken with the CCD camera.

that cells survived the on-chip separation procedure. Simply put, living cells fluoresce red whereas dead cells show no fluorescence.

Cell-containing (10^8 cells ml^{-1}) samples (50 μL) were centrifuged and the supernatant was replaced by 50 μL pre-warmed (37 °C) CellTracker dye (2.5 μM in PBS). The cells were incubated at 37 °C for 30 min and centrifuged again. The dye-containing supernatant was replaced with fresh, pre-warmed medium and the cells were incubated for another 30 min at 37 °C. During this time, the chloromethyl group of the dye undergoes modification in live cells and is secreted from dead cells. Finally, the cells were washed with PBS, spread on microscope slides, and observed immediately.

Results and discussion

The fractions produced by the chip were analyzed with several methods for the purpose of evaluating the separation efficiency. Fig. 4 shows an example of Coulter counter (Beckmann-Coulter) data from the two fractions produced after separation with a filter composed of 15 μm pores. It should be noted that, due to the rarity of cells greater than 15 μm in the original sample, only the number of smaller cells could be effectively determined by Coulter counting. For quantification of larger cells, flow cytometry was required (see below). However, Coulter counter data can still be used as a preliminary evaluation of separation efficiency of cells smaller than 15 μm. The number of small cells that were sorted correctly gave an idea of the purity of the top fraction. The insets in Fig. 4 are confocal images from the sorted fractions. The images were taken after marking both fractions with CD34 antibodies which specifically target progenitor cells. It can be seen that the fraction containing cells that passed through the 15 μm filter (blue line) consists entirely of nonfluorescent cells, mainly erythrocytes. In contrast, the top fraction

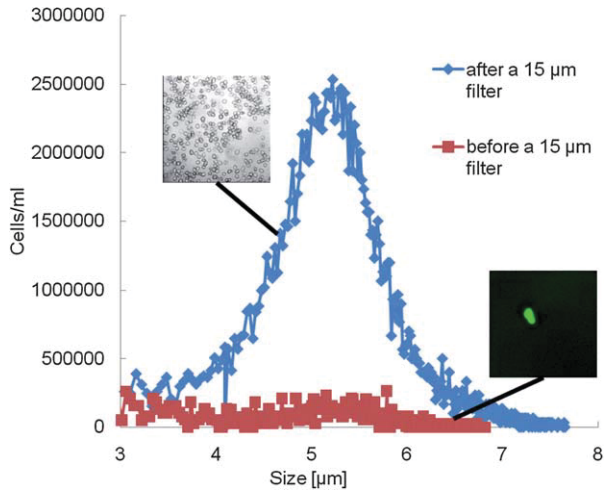

Fig. 4 Coulter counter data for two fractions taken after on-chip separation of full bone marrow. The separation is evaluated by analyzing the number of small cells that can be found in both fractions. The identity of the cells was verified by marking both fractions with an antibody, tagged with FITC (Fluorescein isothiocyanate), that binds to progenitor cells (mouse anti CD34 human). The insets show confocal microscopy images of the bottom fraction (grey image, left) and an antibody-marked stem cell (fluorescence image, right) found in the top fraction.

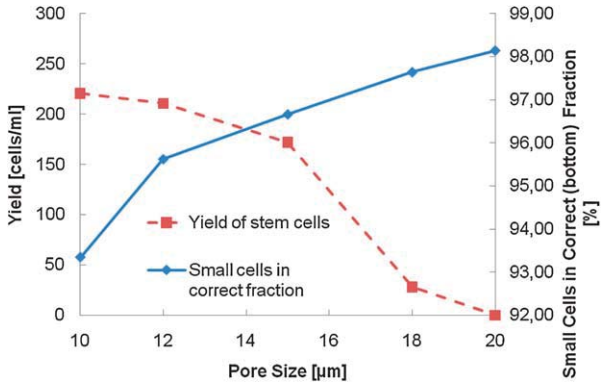

Fig. 5 Optimization of pore size. The yield of stem cells was determined by antibody staining and counting on-chip. The number of small cells that were correctly sorted was evaluated by Coulter counting. The correct pore size can be chosen depending on the throughput, purity and yield that is needed. For standard deviations, see Table 1 below.

(red line) contains far fewer cells and some were identified as fluorescently tagged stem cells.

These Coulter counter data were taken for a range of pore sizes and the percentage of smaller cells that were sorted correctly (which corresponds with the enrichment of the stem cells in the other fraction) was calculated for different separation conditions. After separation with an efficiency of 98%, there are approximately 10^7 cells mL^{-1} remaining in the large cell fraction (determined by Coulter counting). Flow cytometry was performed with anti-CD14 antibody (surface antigen on monocytes) tagged with Texas Red. The amount of monocytes was determined to be about 10% of that so the main impurities are still erythrocytes. Fig. 5 shows the dependency of this percentage on pore size (blue line). As expected, the number of small cells that can pass through the pores increases with pore size. However, as is also expected, the stem cell yield in the top fraction, also plotted in Fig. 5 (red line), decreases with increasing pore size. Because stem cells are deformable to some extent, nearly all stem cells are lost when using pores with 18 and 20 μm diameters. At smaller pore sizes (15 μm or less), stem cell yield is significantly increased. Plots such as this one can be used to decide the optimal sorting conditions for the desired yield and purity of a species. In order to improve clarity, the error bars are not shown in Fig. 5, but can be seen in Table 1, which summarizes several crucial parameters of this experiment.

Another important parameter to consider when using this sorting device is the time required to perform a separation given

Table 1 Summary of the data obtained with the sorting device for different filter sizes and different conditions

Conditions	Efficiency [%]	Throughput [μl min^{-1}]	Yield [Cells/ml]	Viability [%]
10 μm filter	93.3 ± 4.2	2.8 ± 1.1	220 ± 37	93 ± 2
12 μm filter	95.6 ± 3.3	4.7 ± 3.2	210 ± 59	91 ± 5
15 μm filter	96.7 ± 3.8	6.6 ± 3,5	172 ± 60	90 ± 9
18 μm filter	97.6 ± 1.3	7.2 ± 1.5	28 ± 6	94 ± 9
20 μm filter	98.15 ± 1.4	8.8 ± 1.5	0 ± 0	94 ± 7
high throughput	94.4 ± 3.6	17.2 ± 4.9	218 ± 45	92 ± 4
extra flushing	97.6 ± 3.6	8.8 ± 1,6	145 ± 54	91 ± 8

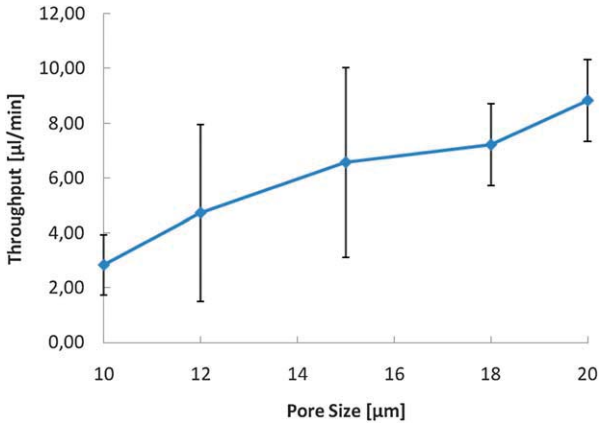

Fig. 6 The throughput of the chip correlated with pore size. Larger pore sizes lead to higher throughputs, as expected. Herein, throughput means the volume that can be processed per minute, which includes the chip handling. The error bars represent the standard deviation obtained from at least four measurements.

a specific pore size, (Fig. 6). The values given for the throughput are not only flow rates but include the time that is needed for the whole experiment. As expected, higher flow rates can be achieved at higher pore sizes. All experiments were performed at 5–10 psi, as suggested by Wei *et al.*[18]), which gives a detailed optimization of this parameter.

To further evaluate this separation method, fractions were also analyzed *via* flow cytometry with a BDFACSCalibur instrument. Fig. 7 shows the results of such an analysis for fractions containing smaller (Fig. 7a–c) and larger (Fig. 7d–f) cells. As can be seen from comparing scatter plots (Fig. 7a and 7d), the second (top) fraction contains far more large cells. Comparing Fig. 7b and 7e, which show the fluorescence correlated with forward scattering, stem cells marked with FITC (green fluorescence red dots in the plots) appear more frequently in the top fraction. By analyzing the number of fluorescent cells (M1 in Fig. 7c and 7f), we found that 93 ± 7% of the stem cells were correctly sorted into the top fraction. When a washing step is included, this number increases to 96 ± 1%. Standard deviations are obtained from four separate experiments. In the fraction containing larger cells, cells other than stem cells are most likely monocytes or smaller cells that were sorted incorrectly.

As shown in Fig. 8, the average viability of cells was above 90% in all experiments. Most cell death is thought to have occurred prior to the experiment rather than during sorting. We expect viability to improve with completely fresh samples. This statement is supported by the fact that when the viability test was performed with an untreated sample it showed nearly the same viability (91 ± 7%) as that found for the processed samples. No significant difference or trend was observed when comparing different separation conditions. This viability is at or above the same range as obtained with density gradient centrifugation with Ficoll, a standard sample preparation and separation used for so hematopoietic stem cells in the literature. However, because our method produces a fraction that contains only hematopoietic stem cells and monocytes, and not all white blood cells (as with the standard method), our method produces purer samples. Depending on the purity needed the filtering chip could be used either for better sample preparation prior to FACS sorting or as the sole sorting technique. Additionally, in contrast to previously

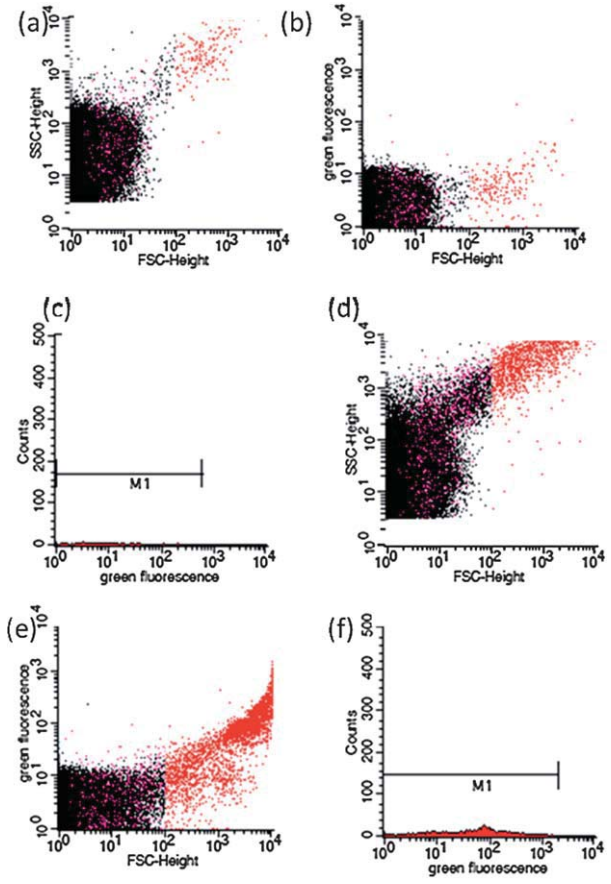

Fig. 7 Flow cytometry data. In order to confirm the enrichment of stem cells, flow cytometry was performed after antibody staining and on-chip sorting. A) thru C) show the bottom cell fraction. D) thru F) show the results obtained from the large-cell fraction containing the FITC-marked progenitor cells.

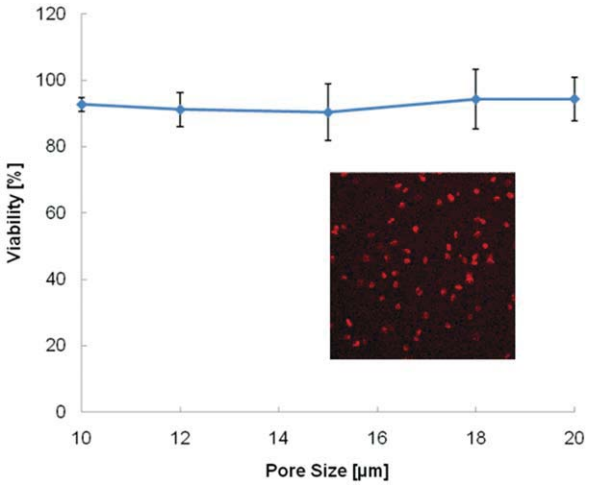

Fig. 8 Viability tests. Viability tests were performed with CellTracker Orange in order to confirm that the cells survive the filtering procedure. No significant trend or difference between different pore sizes was observed. The numbers are based on erythrocytes that survived the procedure, counted under a microscope (see inset). The top fraction was observed as well, and no dead cells were found in that fraction.

shown methods, our chip allows analysis and further on-chip manipulation of cells.

Conclusions

We were able to enrich and quantify human stem cells on-chip from bone marrow samples without any sample pre-treatment. The original chip design and sorting procedure developed in our laboratory by Wei *et al.*[18] were redesigned, improved and applied to the separation of stem cells from bone marrow samples. Different parameters, and their effect on separation efficiency and stem cell yield, were evaluated by flow cytometry and several imaging techniques. The viability of the cells after separation was found to be quite high (>90%), thus verifying our method as a way to produce viable cells.

Acknowledgements

The authors would like to acknowledge the Stanford Nanofabrication Facility where the production of silicon master molds for soft lithography was performed. They would also like to thank the NSF for grant award MCB-0749638-002. We would like to thank the Stanford Hematology Division Tissue Bank for their support.

References

1 T. F. Didar and M. Tabrizian, *Lab Chip*, 2010, **10**, 3043–3053.
2 F.-M. Chen, L.-A. Wu, M. Zhang, R. Zhang and H.-H. Sun, *Biomaterials*, 2011, **32**(12), 3189–3209.
3 S. B. Anderson, C.-C. Lin, D. V. Kuntzler and K. S. Anseth, *Biomaterials*, 2011, **32**(14), 3564–3574.
4 D. Di Carlo, D. Irimia, R. G. Tompkins and M. Toner, *Proc. Natl. Acad. Sci. U. S. A.*, 2007, **104**(48), 18892–18897.
5 M. M. Wang, E. Tu, D. E. Raymond, J. M. Yang, H. Zhang, N. Hagen, B. Dees, E. M. Mercer, A. H. Forster, I. Kariv, P. J. Marchand and W. F. Butler, *Nat. Biotechnol.*, 2005, **23**(1), 83–87.
6 M. A. Burns, B. N. Johnson, S. N. Brahmasandra, K. Handique, J. R. Webster, M. Krishnan, T. S. Sammarco, P. M. Man, D. Jones, D. Heldsinger, C. H. Mastrangelo and D. T. Burke, *Science*, 1998, **282**, 484–487.
7 R. Schirhagl, A. Seifner, F. T. Husain, M. Cichna-Markl, P. A. Lieberzeit and F. L. Dickert, *Sens. Lett.*, 2010, **8**(3), 399–404.
8 T. Sikanen, S. Franssila, T. J. Kauppila, R. Kostainen, T. Kotiaho and R. A. Ketola, *Mass Spectrometry Reviews*, 2010, **29**, 351–391.
9 G. M. Birnbaumer, P. A. Lieberzeit, L. Richter, R. Schirhagl, M. Milnera, F. L. Dickert, A. Bailey and P. Ertl, *Lab Chip*, 2009, **9** (24), 3549–3556.
10 B. Johnsson, S. Löfås and G. Lindquist, *Anal. Biochem.*, 1991, **198**(2), 268–277.
11 J. A. Davis, D. W. Inglis, K. J. Morton, D. A. Lawrence, L. R. Huang, S. Y. Chou, J. C. Sturm and R. H. Austin, *Proc. Natl. Acad. Sci. U. S. A.*, 2006, **103**(40), 14779–14784.
12 A. Y. Fu, C. Spence, A. Scherer, F. H. Arnold and S. R. Quake, *Nat. Biotechnol.*, 1999, **17**(11), 1109–1111.
13 L. R. Huang, E. C. Cox, R. H. Austin and J. C. Sturm, *Science*, 2004, **304**, 987–990.
14 Y. Jiang, M. N. Myers and J. C. Giddings, *J. Liq. Chromatogr. Relat. Technol.*, 1999, **22**(8), 1213–1234.
15 B.-H. Chueh, D. Huh, C. R. Kyrtsos, T. Houssin, N. Futai and S. Takayama, *Anal. Chem.*, 2007, **79**, 3504–3508.
16 S. Thorslund, O. Klett, F. Nikolajeff, K. Markides and J. Bergquist, *Biomed. Microdevices*, 2006, **8**, 73–79.
17 Y. Luo and R. N. Zare, *Lab Chip*, 2008, **8**, 1688–1694.
18 H. Wei, B.-H. Chueh, H. Wu, E. W. Hall, C.-W. Li, R. Schirhagl, J.-M. Li and R. N. Zare, *Lab Chip*, 2011, **11**(2), 238–245.
19 R. J. Jackman, D. C. Duffy, O. Cherniavskaya and G. M. Whitesides, *Langmuir*, 1999, **15**, 2973–2984.
20 M. A. Eddings, M. A. Johnson and B. K. Gale, *J. Micromech. Microeng.*, 2008, **18**(6), 067001.